Check for updates

The impact of structural modification on the electrochromic and electroluminescent properties of D–A–D benzothiadiazole derivatives with a fluorene linker and (Bi)thiophene units†

Roman Ganczarczyk,[a] Renata Rybakiewicz-Sekita, [ID][ab] Magdalena Zawadzka,[c] Piotr Pander, [ID][cde] Przemysław Ledwon, [ID][c] Dawid Nastula[c] and Sandra Pluczyk-Małek [ID] *[cd]

Two donor–acceptor–donor (D–A–D) derivatives of benzothiadiazole (BTD) symmetrically functionalized with dihexylfluorene units serving as a linker between the BTD core and the thiophene (**Th-FBTD**) or bithiophene (**2Th-FBTD**) electron-donating groups were designed, synthesized and comprehensively characterized. Both compounds show high photoluminescence quantum yield (PLQY) both in solution and in the solid state. **Th-FBTD** demonstrates PLQY values of 82% and 96%, whereas **2Th-FBTD** exhibits values of 74% and 97% in DCM and Zeonex, respectively. These compounds were employed as emissive dopants in multilayer solution-processed OLEDs, resulting in green electroluminescence with an emission peak at *ca.* 540 nm. The OLEDs display comparable performance, with a maximum external quantum efficiency of 3.5% for **Th-FBTD** and 2.8% for **2Th-FBTD**. Both **Th-FBTD** and **2Th-FBTD** undergo quasi-reversible electrochemical reduction and irreversible oxidation, giving stable electroactive polymer layers of bipolar character: **p(Th-FBTD)** and **p(2Th-FBTD)**. The electrodeposited polymers undergo one-step reversible reduction and two-step reversible oxidation. Their electrochemical oxidation is accompanied by a reversible color change. Analysis of the optical density difference and coloration efficiency revealed improved electrochromic properties in both visible and near-infrared (NIR) ranges in **p(2Th-FBTD)** compared to that in **p(Th-FBTD)**.

Introduction

Advancements in organic electronics have strengthened the growing interest in research on organic electroactive materials. While a lot of such substances are already known, the continuous development of new technologies requires materials with increasingly sophisticated properties. One of the promising directions are multifunctional or multipurpose materials, which exhibit more than one useful property and can therefore be utilized in a variety of electronic devices or enable fabrication of devices capable of performing multiple functions concurrently.[1–9]

Numerous studies have explored dual electrochromic and emissive compounds; however, these materials predominantly exhibit electrochromism and photoluminescence.[10,11] There are also known materials with both electrochemically controlled coloration and emission.[12–17] Electrochemically controlled (switchable) emission, also called electrofluorochromism, is a property of reversible switching between states with high and low photoluminescence upon electrochemical reduction and/or oxidation.[17–20] However, there are significantly fewer reports regarding dual electrochromic and electroluminescent molecules. This is probably due to the challenges associated with developing an electrochromic system that exhibits efficient electroluminescence at the same time. Nevertheless, certain studies demonstrate that meticulous structural design can yield materials with the desired properties.[21–23]

In recent years, organic electroactive compounds with donor–acceptor–donor (D–A–D) structures have attracted considerable attention due to their properties, which can be tuned by a proper selection of electron-rich and electron-deficient groups.[21] The mode of linking donor and acceptor groups allows adjusting the magnitude of interaction between them.

[a] Faculty of Chemistry, Warsaw University of Technology, Warsaw, Poland
[b] Cardinal Stefan Wyszynski University, Faculty of Mathematics and Natural Sciences, School of Exact Sciences, Warsaw, Poland
[c] Faculty of Chemistry, Silesian University of Technology, Gliwice, Poland. E-mail: sandra.pluczyk-malek@polsl.pl
[d] Centre for Organic and Nanohybrid Electronics, Silesian University of Technology, Gliwice, Poland
[e] Department of Physics, Durham University, Durham, UK
† Electronic supplementary information (ESI) available. See DOI: https://doi.org/10.1039/d4tc01583e

This journal is © The Royal Society of Chemistry 2024

J. Mater. Chem. C, 2024, **12**, 15201–15214 | **15201**

This in turn exerts a remarkable influence on the optical, electrochemical, and spectroelectrochemical properties of the resulting material.[24–28]

Benzothiadiazoles (BTDs) show strong electron-withdrawing properties and hence may undergo reversible electrochemical reduction.[29] Additionally, they are widely used as a fluorophore.[30] Furthermore, the use of benzothiadiazole as a building block was found to result in multifunctional materials. For instance, Koldemir *et al.* reported a polymer based on BTDs which they used in a dual electrochromic/electroluminescence device and additionally demonstrated satisfactory photovoltaic performance using this material.[21] On the other hand, fluorene serves as a notable building block known for its promising performance in electrochromic and electroluminescent devices.[21,22] Finally, thiophenes and their derivatives are renowned as electron-donating materials typically exhibiting stable electrochromism.[31–33] Additionally, thiophene derivatives with an unsubstituted α-position are often active in electrochemical polymerization facilitating deposition of electrochromic layers.[31,34]

Taking into account all the abovementioned points, we have decided to synthesize D–A–D derivatives of benzothiadiazole symmetrically functionalized with dihexylfluorene serving as a linker between the BTD core and thiophene (**Th-FBTD**) or bithiophene (**2Th-FBTD**) units. In this work, we present the results of electrochemical, spectroscopic, and UV-Vis spectroelectrochemical characterization of these two new D–A–D multifunctional materials. The investigated molecules exhibit high fluorescence quantum yield both in the solid state and in solution. They can be used as emissive dopants in multilayer solution-processed OLEDs, demonstrating promising performance. Additionally, both molecules undergo electrochemical polymerization yielding stable electrochromic layers. Our comprehensive analysis demonstrated that incorporating an additional thiophene ring in the monomer structure has a positive impact on the electrochromic properties of the electrodeposited polymeric layer. The obtained polymer **p(2Th-FBTD)** exhibits improved stability, optical density difference, and coloration efficiency in the visible and near-infrared (NIR) range compared to **p(Th-FBTD)** with bithiophene units. The benzothiadiazole derivatives featuring a fluorene linker and thiophene or bithiophene units proposed in this study have demonstrated enhanced coloration efficiency compared to

various donor–acceptor type polymers, including those based structurally on fluorene,[35] thiophene,[36] and benzothiadiazole.[37] This observation further underscores the substantial potential of our materials.
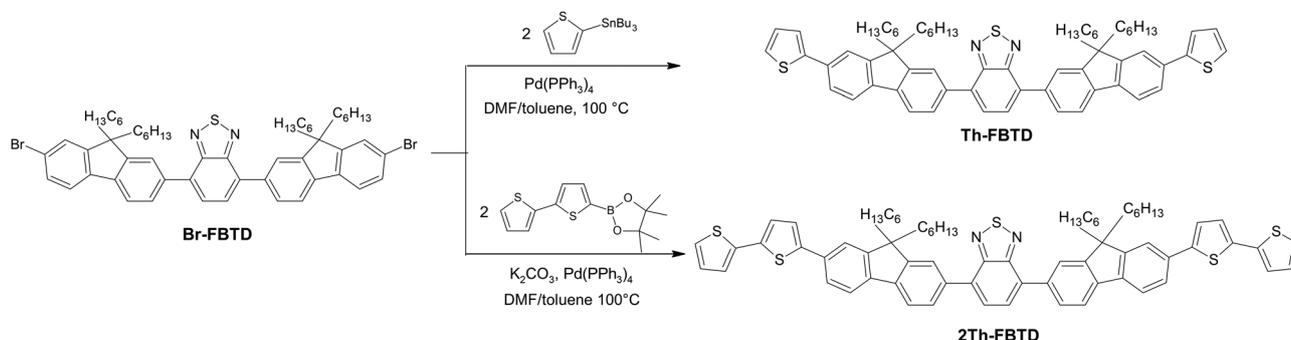
Results and discussion

Synthesis

Both 4,7-bis(9,9-dihexyl-7-(thiophen-2-yl)-9H-fluoren-2-yl)benzo-[c][1,2,5]thiadiazole (**Th-FBTD**) and 4,7-bis(7-([2,2′-bithiophen]-5-yl)-9,9-dihexyl-9H-fluoren-2-yl)benzo[c][1,2,5]thiadiazole (**2Th-FBTD**) were prepared using a similar synthetic approach. The synthesis of the common core unit, 4,7-bis(7-bromo-9,9-dihexyl-9H-fluoren-2-yl)benzo[c][1,2,5]thiadiazole (**Br-FBTD**), was achieved in three steps according to known procedures or their modifications.[38] First, one of the bromine atoms of the commercially available 9,9-dihexyl-2,7-dibromofluorene was exchanged with trimethylsilyl unit under previously reported conditions.[39] **BrFTMS** (7-bromo-9,9-dihexyl-9H-fluoren-2-yl)trimethylsilane was then coupled *via* a Suzuki–Miyaura reaction with 2,1,3-benzothiadiazole-4,7-bis(boronic acid pinacol ester) to form 4,7-bis(9,9-dihexyl-7-(trimethylsilyl)-9H-fluoren-2-yl)benzo[c][1,2,5]thiadiazole (**TMS-FBTD**). In the next step, the peripheral trimethylsilyl groups were substituted by bromine to afford the key intermediate compound 4,7-bis(7-bromo-9,9-dihexyl-9H-fluoren-2-yl)benzo[c][1,2,5]thiadiazole (**Br-FBTD**) in high yield (94%). Finally, **Br-FBTD** was used in Stille or Suzuki–Miyaura coupling with appropriate electron-rich terminal groups: 2-(tributylstannyl)thiophene or 2,2′-bithiophene-5-boronic acid pinacol ester to obtain **Th-FBTD** and **2Th-FBTD**, respectively. The synthetic procedure is summarized in Scheme 1. Further synthetic details can be found in the ESI† which in addition contains all spectroscopic (¹H NMR and ¹³C NMR) data (Fig. S1–S5, ESI†).

Thermal analysis

Thermal stability of the obtained compounds was examined using thermogravimetric analysis (TGA) and differential scanning calorimetry (DSC). The experimental data are presented in Fig. 1. Both **Th-FBTD** and **2Th-FBTD** exhibit endothermic transitions associated with melting at 114 °C and 216 °C,

Scheme 1 Synthetic route for preparation of **Th-FBTD** and **2Th-FBTD**.

15202 | *J. Mater. Chem. C*, 2024, **12**, 15201–15214

This journal is © The Royal Society of Chemistry 2024

respectively. High decomposition temperatures, T_d, corresponding to a 5% weight loss, have been observed: $T_d = 442$ °C in **2Th-FBTD** and $T_d = 425$ °C in **Th-FBTD**, indicating excellent thermal stability.

Calculations

We use density functional theory (DFT) and time-dependent DFT (TD-DFT) implemented in Orca 4.2.1[40–42] to model the electronic excited state properties of **Th-FBTD** and **2Th-FBTD**. The molecules adopt a geometry in which the peripheral thiophene (**Th-FBTD**) and bithiophene (**2Th-FBTD**) subunits are nearly coplanar (dihedral angle $\sim 20°$) with the linking fluorenes. The fluorene units then form a larger torsion angle with the central benzothiadiazole moiety, *ca.* 40°, which allows for partial conjugation. The highest occupied natural transition orbitals (HONTOs) for the S_1 state are distributed over the benzene fragment of the benzothiadiazole unit as well as the fluorene units, with negligible contributions from the thiophenes/bithiophenes. However, the thiophene/bithiophene units clearly alter the electron density on the fluorenes through σ-donation. The lowest unoccupied natural transition orbitals (LUNTOs) for the S_1 state are localized predominantly at the benzothiadiazole acceptor (Fig. 2). The lowest excited singlet state (S_1) displays a large transition oscillator strength $f(S_0 \rightarrow S_1) \approx 1$–2 in both molecules, thanks to the significant overlap of the frontier natural transition orbitals (NTOs) mainly at the benzene fragment of the benzothiadiazole unit. This suggests that **Th-FBTD** and **2Th-FBTD** should display a highly fluorescent behavior.[43] The $S_0 \rightarrow S_1$ (3.24 eV for **Th-FBTD** and 3.21 eV for **2Th-FBTD**) transition can be assigned a hybrid local and charge transfer (CT) character, $\pi\pi^* +$ CT, due to the electron density partly shifting from the fluorene units inwards to the acceptor. Another transition with a significant ($f > 1$) oscillator strength is $S_0 \rightarrow S_3$ (4.19 eV for **Th-FBTD** and 3.85 eV for **2Th-FBTD**) with a similarly large overlap of the respective NTOs (see HONTOs and LUNTOs for the S_3 state in Fig. S6 in the ESI†). Simulated absorption spectra of **Th-FBTD** and **2Th-FBTD** are presented in the ESI,† Fig. S7, singlet and triplet excitation energies for both molecules are listed in Tables S1 and S2 (ESI†).
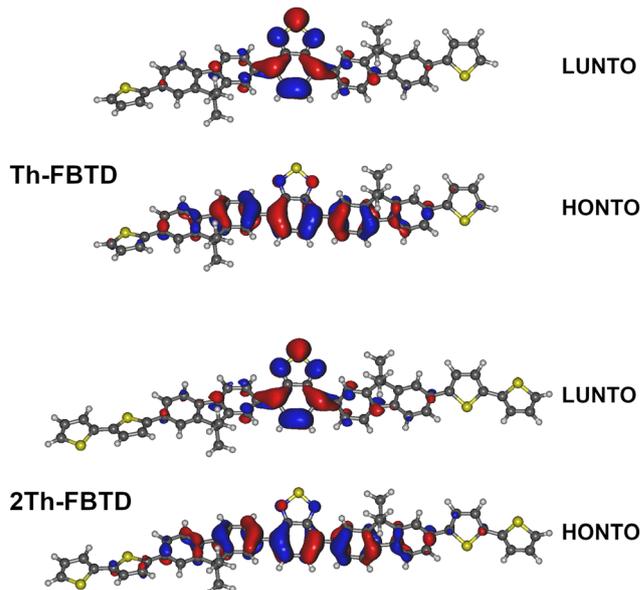

Fig. 2 The highest occupied and lowest unoccupied natural transition orbitals (NTOs): HONTO and LUNTO, respectively, for the S_1 state, calculated at the ground state (S_0) geometry of **Th-FBTD** and **2Th-FBTD**, using the CAM-B3LYP/def2-SVP/CPCM(CH$_2$Cl$_2$) level of theory.

UV-Vis absorption and fluorescence spectroscopy

To investigate the optical properties of the studied compounds, we used spectrophotometry and fluorescence spectroscopy. The normalized UV-Vis absorption spectra of **Th-FBTD** and **2Th-FBTD**, recorded in dichloromethane (DCM), are shown in Fig. 3 (dashed lines). We observe two main absorption bands within the optical window. DFT calculations suggest that both bands display a hybrid $\pi\pi^* +$ CT character which is consistent with the experimental behavior of the two luminophores. The energetically lowest transition is centered at *ca.* 430 nm for both luminescent molecules. However, the onset of this absorption band is slightly red-shifted in **2Th-FBTD** compared to **Th-FBTD**, leading to a more narrow energy gap in the former: 2.51 eV (**2Th-FBTD**) and 2.55 eV (**Th-FBTD**). A more significant shift can be observed for the higher energy band as in this case, it is centered at 345 nm in **Th-FBTD** and at 371 nm in **2Th-FBTD** (Table 1).
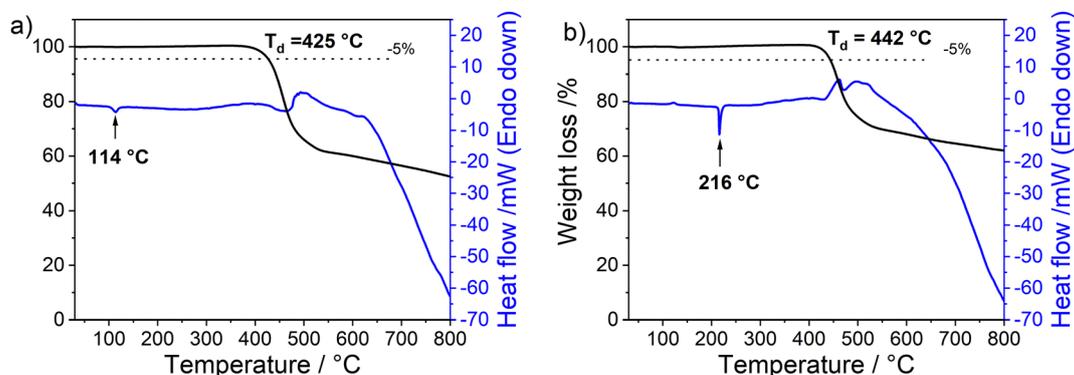

Fig. 1 TGA and DSC curves for (a) **Th-FBTD** and (b) **2Th-FBTD**.

This journal is © The Royal Society of Chemistry 2024

J. Mater. Chem. C, 2024, **12**, 15201–15214 | **15203**
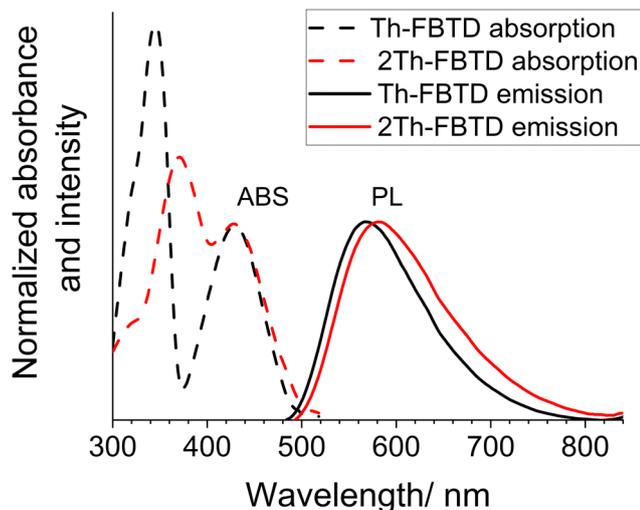
Fig. 3 UV-Vis absorption spectra (dashed lines) and normalized photo-luminescence spectra (continuous lines) of investigated benzothiadiazole derivatives **Th-FBTD** and **2Th-FBTD** in $c = 10^{-6}$ M DCM solution. The spectra are normalized to the lowest absorption band of each respective molecule.

The normalized fluorescence spectra recorded in DCM are shown in Fig. 3 (continuous lines). These spectra consist of one broadband signal centered at 568 nm for **Th-FBTD** and 582 nm for **2Th-FBTD**. The fluorescence spectra of **2Th-FBTD** exhibit a bathochromic shift as compared with **Th-FBTD**, which is in line with the behaviour of the absorption spectra. This shift is likely attributed to the stronger σ-donating effect of bithiophenes relative to thiophenes on the HOMO energy. Additionally, the Stokes shift for **2Th-FBTD** (6128 cm^{-1}) is greater than that for **Th-FBTD** (5704 cm^{-1}). Such large Stokes shifts are commonly observed in D–A–D structures and indicate the intramolecular charge transfer character of the lowest excited state.[44,45] Moreover, this substantial Stokes shift may also be linked to significant geometry relaxation of these molecules in the excited state.[46] Furthermore, the large Stokes shift results in a relatively small overlap between absorption and emission (indeed, a relatively negligible overlap is observed in Fig. 3). This characteristic feature is advantageous in solid-state applications, such as in organic light-emitting diodes (OLEDs), as it reduces losses due to re-absorption of electroluminescence, potentially leading to higher external quantum efficiency (EQE).

Both compounds exhibit high photoluminescence quantum yields (PLQY) in solution and in a solid-state polymer matrix. Notably, the PL spectra in solution display a visible positive solvatochromism between dichloromethane and toluene. Additionally, the emission spectra in Zeonex for both investigated compounds are blue-shifted with respect to those recorded in toluene. Furthermore, the emission spectra in Zeonex are more narrowband than in solution, which is attributed to the rigid environment of the polymer matrix and its generally low polarity (Fig. S8 and Table 1, ESI†).[47,48] It is observed that both compounds show higher PLQY in the solid-state matrix than in dilute solution, with PLQYs reaching as high as 96% and 97% for **Th-FBTD** and **2Th-FBTD**, respectively. In DCM and toluene solutions, **Th-FBTD** exhibits higher PLQY compared to **2Th-FBTD**. This difference is especially evident in toluene, where **Th-FBTD** shows a PLQY of 95% whereas for **2Th-FBTD**, it reaches 79%. This discrepancy is also reflected in the fluorescence lifetime (τ) of the two luminophores in the same solvent. **Th-FBTD** displays τ of 3.4 ns, corresponding to a radiative rate constant k_r of 2.8×10^8 s^{-1}, while for **2Th-FBTD**, τ is 2.6 ns with k_r being 3.0×10^8 s^{-1}. As the two radiative rates are nearly identical, it indicates that a slight shortening of τ in **2Th-FBTD** with respect to **Th-FBTD** is due to faster non-radiative deactivation in the former (Fig. 4). In general, the decay lifetimes and corresponding radiative rates of **Th-FBTD** and **2Th-FBTD** indicate their strongly fluorescence behaviour being a consequence of the strongly allowed nature of the $S_0 \rightarrow S_1$ transition indicated by the large absorption coefficient of the lowest electronic transition, $\varepsilon > 10^4$ M^{-1} cm^{-1}.[43]

Electrochemical properties

We use cyclic voltammetry (CV) to analyze the electrochemical properties of presented molecules. Both compounds undergo quasi-reversible reduction and irreversible oxidation (Fig. 5). We estimate the electron affinity (EA), the ionization potential (IP), and the electrochemical energy gap ($E_{g,el}$) using the values of onset potentials, as summarized in Table 2. The reduction potential of **2Th-FBTD** (−2.03 V) is only slightly lower than the reduction potential of **Th-FBTD** (−1.98 V), indicating a negligible impact of the donor on the reduction potential of the BTD acceptor unit. Notably, the reduction potential of **Th-FBTD** is the same as for earlier reported benzothiadiazole derivatives with thiophene units directly attached to the BTD core (i.e. without the fluorene spacer),[49] suggesting that the fluorene

Table 1 Optical properties of **Th-FBTD** and **2Th-FBTD**

Compound	Solvent/matrix	$\lambda_{abs}{}^a$/nm (ε^b/10^4 M^{-1} cm^{-1})	$\lambda_{em}{}^c$/nm	FWHM$_{em}{}^d$/nm	PLQY^e/%
Th-FBTD	DCM	345 (7.72); 429 (3.81)	568	112	82
	Toluene	344 (6.08); 431 (2.96)	539	93	95
	Zeonex	—	529	74	96
2Th-FBTD	DCM	371 (9.05); 429 (6.75)	582	128	74
	Toluene	370 (7.62); 433 (5.80)	547	95	79
	Zeonex	—	535	72	97

^{a} Absorption spectrum maxima. ^{b} Molar attenuation coefficient. ^{c} Fluorescence spectrum maxima. ^{d} Full width at half maximum of the PL spectrum. ^{e} Photoluminescence quantum yield.

15204 | *J. Mater. Chem. C*, 2024, **12**, 15201–15214

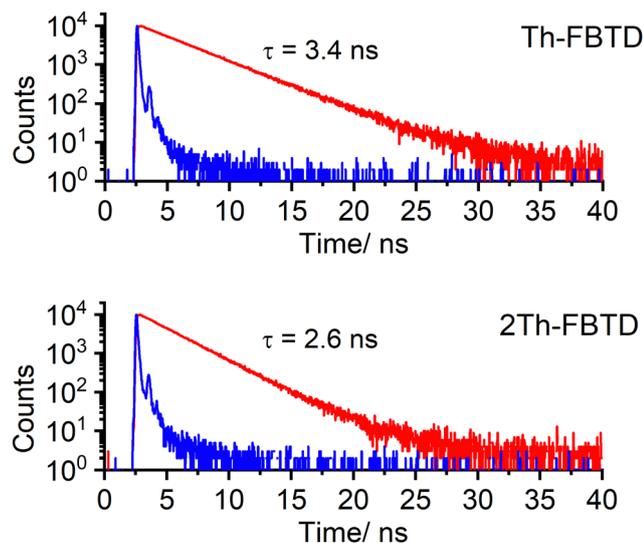This journal is © The Royal Society of Chemistry 2024

Fig. 4 Photoluminescence decay of **Th-FBTD** and **2Th-FBTD** in a degassed dilute ($c = 10^{-6}$ M) toluene solution: TCSPC decay traces with collection at $\lambda_{PL} = 550$ nm (red lines); instrument response function, IRF (blue lines).

linker does not influence the reduction process of thiophene-benzothiadiazole derivatives. However, **Th-FBTD** displays a slightly higher oxidation potential compared to the previously reported analogue.[49] These findings are consistent with the NTOs presented in Fig. 2. **2Th-FBTD** exhibits a narrower energy gap (2.50 eV) due to the presence of stronger electron-donating bithiophene moieties. The bithiophene unit acts as a stronger σ-donor against the fluorene linker, hence reducing the oxidation potential of **2Th-FBTD** (0.69 V) with respect to **Th-FBTD** (0.87 V). The signals recorded in the cathodic half-cycle at 0.75 V and 0.45 V for **Th-FBTD** and 0.50 V and 0.25 V for **2Th-FBTD** are connected with the reduction of products generated during irreversible electrochemical oxidation of investigated molecules.

OLED devices

To demonstrate the potential application of **Th-FBTD** and **2Th-FBTD**, they have been used as emissive dopants in multilayer solution-processed OLEDs, denoted Dev 1 and Dev 2, respectively. Device characteristics are presented in Fig. 6 and Table 3, with supplementary data provided in the ESI† (Fig. S9 and S10). The best results have been obtained with a device structure employing high molecular weight ($M = 1.1 \times 10^6$ Da) poly(N-vinylcarbazole) (PVKH) as a hole transport and electron-blocking layer and a blend of low molecular weight ($M = 9 \times 10^4$ Da) poly(N-vinylcarbazole) (PVK) and 5-(4-tert-butylphenyl)-1,3,4-oxadiazole (PBD) as the host (AFM images of the host blend are presented in Fig. S12, ESI†): ITO|AI4083 (30 nm)|PVKH (10 nm)|PVK : PBD (50 : 50 w/w) co 5% **Th-FBTD** or **2Th-FBTD** (30 nm)|TPBi (45 nm)|LiF (0.8 nm)|Al (100 nm) (Fig. S13, ESI†). This general device architecture has previously demonstrated excellent electrical and electroluminescence performance with green- and yellow-luminescent dopants.[50] Dev 1 and Dev 2 exhibit green electroluminescence with maxima at 538 nm and 543 nm, respectively. The turn-on voltage (V_{ON}) for both devices is at around 6 V. The overall performance is similar for both devices, with maximum EQE values at 3.5% and 2.8% for Dev 1 and Dev 2, respectively. Dev 2 demonstrates a larger maximum luminance, 7100 cd m^{-2}, than Dev 1 with 6400 cd m^{-2}.

Electrochemical polymerization and properties of the electrodeposited layer

Irreversible oxidation of both compounds is associated with their activity in the electrochemical polymerization process due to the presence of thiophene units with unsubstituted α-position in the monomer structures. In subsequent CV cycles, a new signal arises at lower potentials than those for monomeric **Th-FBTD** and **2Th-FBTD**, and with each consecutive CV scan, these signals grow in intensity, indicating the deposition of an electroactive layer on the working electrode surface (Fig. 7). Generally speaking, polymerization of thiophene
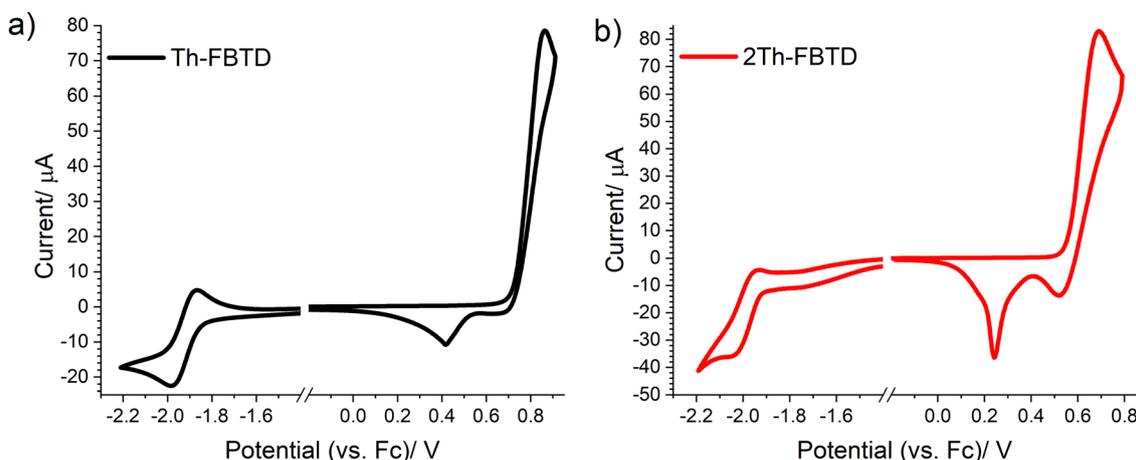

Fig. 5 Cyclic voltammograms recorded for 1.0 mM solution of (a) **Th-FBTD** and (b) **2Th-FBTD** in 0.1 M Bu$_4$NPF$_6$/DCM electrolyte. Scan rate 0.1 V s^{-1}.

This journal is © The Royal Society of Chemistry 2024

J. Mater. Chem. C, 2024, **12**, 15201–15214 | **15205**

Table 2 Electrochemical data together with values of optical energy gap of the studied compounds

Compound	E_{ox}^{a}/V	E_{red}^{b}/V	$E_{ox}^{onset\ c}$/V	$E_{red}^{onset\ d}$/V	IP^{e}/eV	EA^{f}/eV	Eg$_{el}^{g}$/eV	λ_{onset}^{h}/nm	Eg$_{opt}^{i}$/eV
Th-FBTD	0.87	−1.98	0.79	−1.74	5.88	−3.31	2.57	486	2.55
2Th-FBTD	0.69	−2.03	0.55	−1.89	5.71	−3.21	2.50	493	2.51

^{a} Anodic (oxidation) peak potential. ^{b} Cathodic (reduction) peak potential. ^{c} Oxidation onset potential. ^{d} Reduction onset potential. ^{e} Ionization potential: IP = E_{ox}^{onset} + 5.1/eV. ^{f} Electron affinity: EA = −(E_{red}^{onset} + 5.1)/eV. ^{g} Electrochemical energy gap: Eg$_{el}$ = |−IP − EA|/eV. ^{h} UV-Vis absorption onset wavelength. ^{i} Optical energy gap: Eg$_{opt}$ = $\frac{1240}{\lambda_{onset}}$/eV.
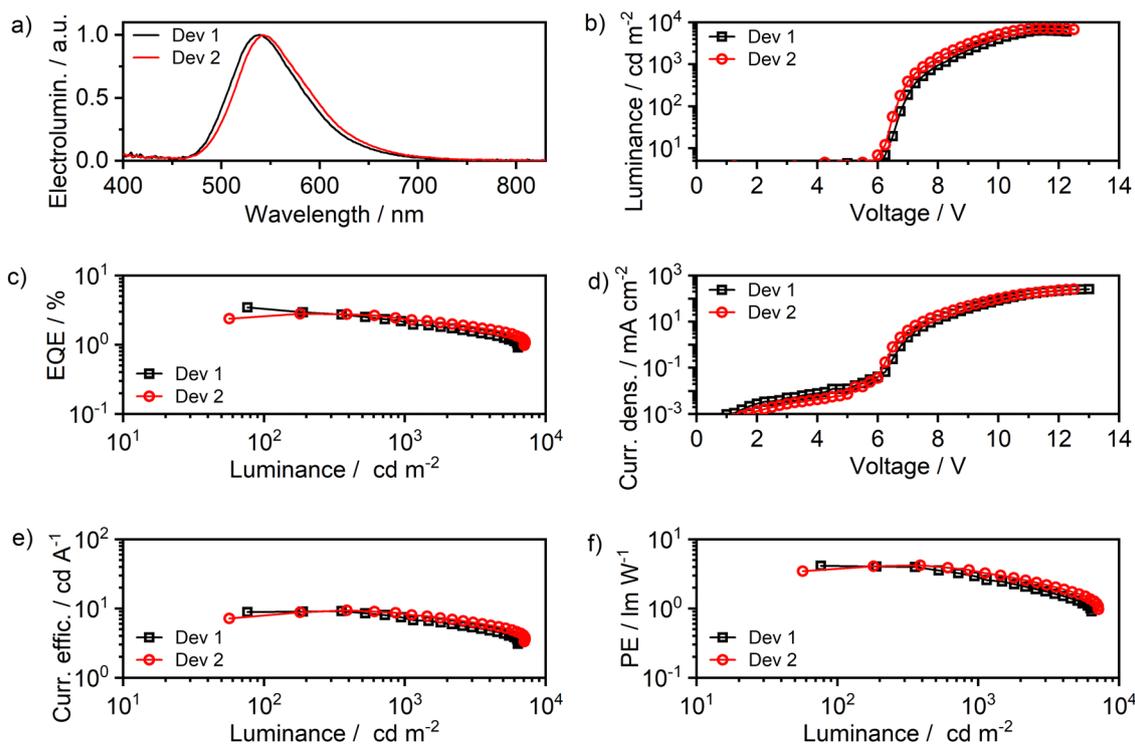

Fig. 6 Characteristics of OLED devices 1 (using **Th-FBTD** as an emitter) and 2 (using **2Th-FBTD** as an emitter): (a) electroluminescence spectra at 10 V; (b) luminance *vs.* voltage; (c) external quantum efficiency (EQE) *vs.* luminance; (d) current density *vs.* voltage; (e) current efficiency *vs.* luminance; (f) power efficiency (PE) *vs.* luminance.

Table 3 Characteristics of OLED devices 1 and 2

	Dev 1	Dev 2
Emitter	**Th-FBTD**	**2Th-FBTD**
V_{ON}^{a}/V	6.5	6.5
L_{max}^{b}/cd m^{-2}	6400	7100
λ_{EL}^{c}/nm	538	543
CIE 1931 $(x, y)^{d}$	(0.36, 0.58)	(0.38, 0.57)
FWHM^{e}/nm	85	85
CE$_{max}^{f}$/cd A^{-1}	9.2	9.4
PE$_{max}^{g}$/lm W^{-1}	4.1	4.2
EQE$_{max}^{h}$/%	3.5	2.8

^{a} Turn-on voltage at 10 cd m^{-2}. ^{b} Maximum luminance. ^{c} Electroluminescence spectrum maxima. ^{d} Colour coordinates of electroluminescence spectrum as defined in International Commission on Illumination colour space CIE 1931. ^{e} Full width at half maximum. ^{f} Maximum current efficiency. ^{g} Maximum power efficiency. ^{h} Maximum external quantum efficiency.

derivatives occurs through the bonding of the monomer units at the α- or β-position in thiophene rings; however, the α-position in thiophenes has been proven to be the most reactive in the polymerization process.[51–53] Hence, the monomers predominantly form oligomers or polymers through the α–α linkage between the thiophene units (Fig. S14, ESI†). Oxidation of monomers leads to creation of reactive radical cations. These reactive species then couple with each other forming insoluble oligo- and polymeric products that deposit on the working electrode surface.[52,54]

The electrochemical properties of electrodeposited polymeric layers were investigated through CV measurements in a monomer-free electrolyte solution. Both deposited materials undergo a reversible one-step electrochemical reduction and a two-step reversible oxidation (Fig. 8). Similar to the respective monomers **Th-FBTD** and **2Th-FBTD**, the reduction process is independent of the donor unit, as the reduction peaks for both **p(Th-FBTD)** and **p(2Th-FBTD)** are observed at nearly identical potentials: −1.94 V for **p(Th-FBTD)** and −1.96 V for **p(2Th-FBTD)** (Table 4). It is noteworthy that these values are only

15206 | *J. Mater. Chem. C*, 2024, **12**, 15201–15214

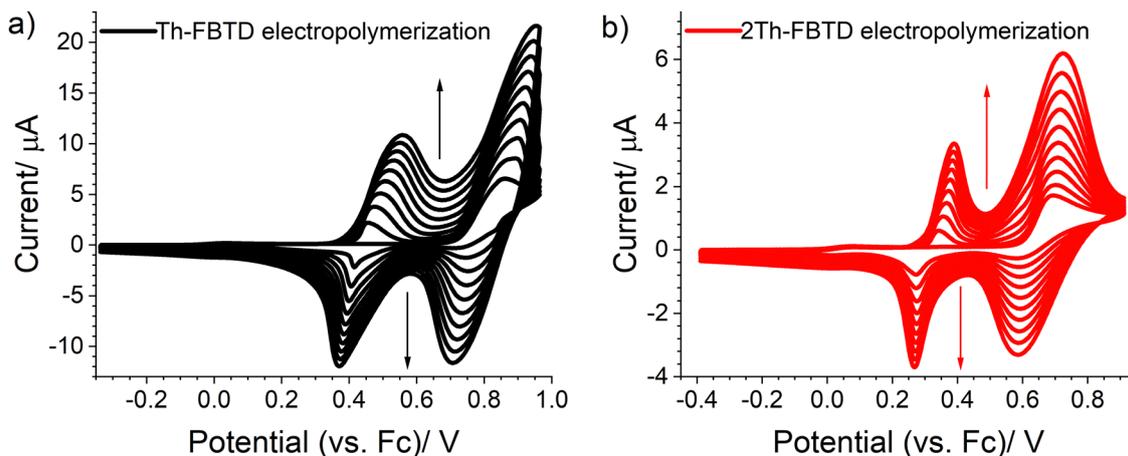This journal is © The Royal Society of Chemistry 2024

Fig. 7 Potentiodynamic electropolymerization of (a) **Th-FBTD** and (b) **2Th-FBTD** (0.5 mM solutions), using a platinum working electrode immersed in 0.1 M Bu$_4$NPF$_6$/DCM electrolyte (10 cycles). Scan rate 0.1 V s^{-1}. The arrows indicate the direction of the current increase in the voltammograms.

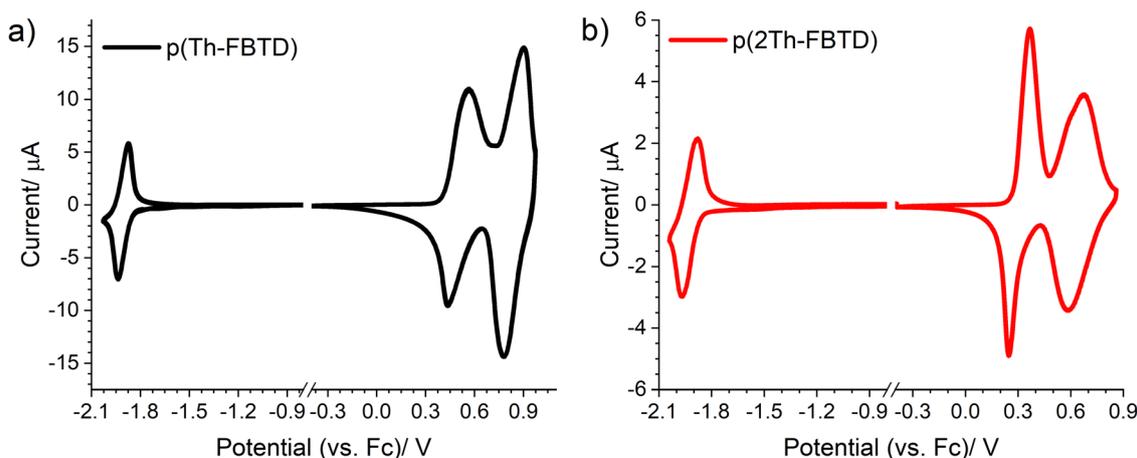Fig. 8 Cyclic voltammograms of the electrodeposited layers of (a) **p(Th-FBTD)** and (b) **p(2Th-FBTD)**, in a monomer-free 0.1 M Bu$_4$NPF$_6$/DCM electrolyte solution. Scan rate 0.1 V s^{-1}.

Table 4 Summary of the key electrochemical data for electrodeposited films together with values of the optical energy gap

Compound	E_{ox}^{a}/V	E_{red}^{b}/V	$E_{ox}^{onset\ c}$/V	$E_{red}^{onset\ d}$/V	IP^{e}/eV	EA^{f}/eV	Eg$_{el}^{g}$/eV	λ_{onset}^{h}/nm	Eg$_{opt}^{i}$/eV
p(Th-FBTD)	0.56; 0.90	−1.94	0.41 0.69	−1.85	5.51	−3.25	2.26	540	2.30
p(2Th-FBTD)	0.37; 0.68	−1.96	0.28 0.45	−1.87	5.38	−3.23	2.15	563	2.20

^{a} Anodic (oxidation) peak potential. ^{b} Cathodic (reduction) potential. ^{c} Oxidation onset potential. ^{d} Reduction onset potential. ^{e} Ionization potential: IP = E_{ox}^{onset} + 5.1/eV. ^{f} Electron affinity: EA = $-(E_{red}^{onset}$ + 5.1)/eV. ^{g} Electrochemical energy gap: Eg$_{el}$ = |−IP − EA|/eV. ^{h} UV-Vis absorption onset wavelength. ^{i} Optical energy gap: Eg$_{opt}$ = $\dfrac{1240}{\lambda_{onset}}$/eV.

marginally higher than for the respective monomers. A more significant difference is observed for oxidation processes. The oxidation of **p(2Th-FBTD)** occurs at a lower potential (0.37 V) in contrast to **p(Th-FBTD)** (0.56 V). Specifically, the maximum of the first oxidation step for **p(2Th-FBTD)** occurs at a potential approximately 0.30 V lower than for the corresponding

2Th-FBTD monomer. A similar difference in oxidation potential is observed between **p(Th-FBTD)** and **Th-FBTD** (compare Tables 2 and 4). This observation indicates that **p(2Th-FBTD)** exhibits higher conjugation of the thiophene units relative to **p(Th-FBTD)** (*i.e.* four *vs.* two linked thiophene units). Furthermore, polymers display a significant alteration in their HOMO

concerning the respective monomers, while the LUMO remains virtually unchanged. Despite the electrochemical behavior similarities between **Th-FBTD** and other reported thiophene-benzothiadiazole derivatives,[49] the incorporation of fluorene into the structure results in significant changes in the electrochemical response of the electropolymerized layers. In the earlier reported derivative, where benzothiadiazole directly links with thiophene rings, the electrodeposited layer undergoes one-step electrochemical oxidation, and the reduction process for this layer is shifted to a higher potential by *ca.* 0.20 V compared with the starting monomer.[49] In this study, the oxidation of **p(Th-FBTD)** and **p(2Th-FBTD)**, is a two-step process, and the reduction potential of electrodeposited layers remains almost identical to that of the starting monomers. This implies that the inclusion of fluorene moieties separating the thiophene or bithiophene units from the benzothiadiazole core effectively isolates electronically the peripheral thiophene or bithiophene units. This finding is consistent with the outcomes derived from DFT calculations.

UV-Vis absorption spectroscopy and spectroelectrochemistry of p(Th-FBTD) and p(2Th-FBTD)

The UV-Vis absorption spectra of **p(Th-FBTD)** and **p(2Th-FBTD)** electrochemically deposited on an ITO electrode are shown in Fig. 9. Notably, the absorption spectra of the polymeric layers are clearly red shifted in respect to the monomers. We attribute the lowest absorption band to a hybrid ππ* + CT transition as in the respective monomers. Importantly, the absorption band is more profoundly red shifted in **p(2Th-FBTD)** (480 mm) than in **p(Th-FBTD)** (455 nm), which is associated with a larger number of conjugated thiophene units in **p(2Th-FBTD)**. Values of energy gap calculated from electrochemical (Eg_{el}) and

Fig. 9 UV-Vis absorption spectra of electrodeposited **p(Th-FBTD)** (black continuous line) and **p(2Th-FBTD)** (red continuous line) on ITO/glass. Spectra are normalized to the lowest absorption band. UV-Vis absorption spectra of monomers in DCM solutions are shown in dashed lines for reference.

spectroscopic (Eg_{opt}) measurements are nearly identical (Table 4), exhibiting a consistent trend. In particular, the energy gap of **p(2Th-FBTD)** is lower by 0.10 eV compared to **p(Th-FBTD)**. Electropolymerization leads to materials with lower energy gap relative to the respective monomers; however, the change is more significant for **p(2Th-FBTD)** (ΔEg_{el} = 0.35 eV and ΔEg_{opt} = 0.31 eV) than in the case of **p(Th-FBTD)** (ΔEg_{el} = 0.30 eV and ΔEg_{opt} = 0.25 eV), which is directly linked to the proposed structure of these polymers. We believe that **p(Th-FBTD)** comprises two repeating units of thiophene, while **p(2Th-FBTD)** contains four such units (Fig. S14, ESI†).

The UV-Vis spectroelectrochemical characterization of the obtained polymeric layers was conducted in terms of their electrochromic properties. The study was performed in a designated spectroelectrochemical cell filled with a monomer-free electrolyte solution. The UV-Vis absorption spectra recorded during the electrochemical oxidation of **p(Th-FBTD)** and **p(2Th-FBTD)** are depicted in Fig. 10. We note a two-stage nature of this process, consistent with the CV studies. Upon oxidation, the absorption band at 455 nm and 480 nm associated with the neutral form of **p(Th-FBTD)** and **p(2Th-FBTD)**, respectively, gradually reduces in intensity and lightly blue shifts. Simultaneously, a new band arises in the first oxidation step at *ca.* 650 nm for **p(Th-FBTD)** and 685 nm for **p(2Th-FBTD)**, which in the second oxidation step slightly red shifts, but also weakens to the point it no longer displays a distinctive maximum. A new, wide absorption band with a maximum exceeding 1000 nm appears in the second oxidation step in both layers. In general, **p(Th-FBTD)** and **p(2Th-FBTD)** behave similarly except that the absorption band associated with the first oxidation step of **p(Th-FBTD)** is slightly blue shifted (*i.e.* 650 nm) compared to the corresponding band in **p(2Th-FBTD)**, likely due to fewer thiophene units participating in oxidation in **p(Th-FBTD)** than in the latter polymer. Importantly, the electrochromic behavior of both polymers is fully reversible and reproducible in successive on–off cycles, a feature that is further discussed in detail in the following section.

Electrochromism

We carried out measurements of the electrochromic properties in the anodic range, taking into account the reversible nature of the electrochemical oxidation processes of electrodeposited **p(Th-FBTD)** and **p(2Th-FBTD)** layers. The spectra and kinetic curves recorded *in situ* during the electrochemical measurements presented in this section relate to p-type doping and de-doping of polymer films. They reveal reversible changes in the absorbance of the studied polymers in the UV-Vis-NIR range.

Photographs of polymers deposited on ITO electrodes were captured during electrochemical oxidation, and the results are presented in Fig. 11. The CVs recorded in the spectroelectrochemical cell differ from those recorded in conventional electrochemical cells due to the greater influence of layer conductivity and diffusion limitations in this setup. Noticeable color changes are observed for different oxidation states. **p(Th-FBTD)** is yellow in its neutral state, transitioning to green in the first oxidation state, followed by blue, and finally gray in
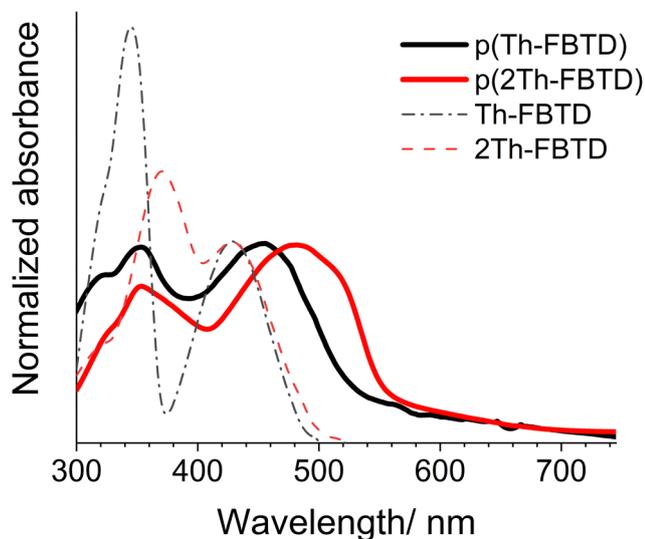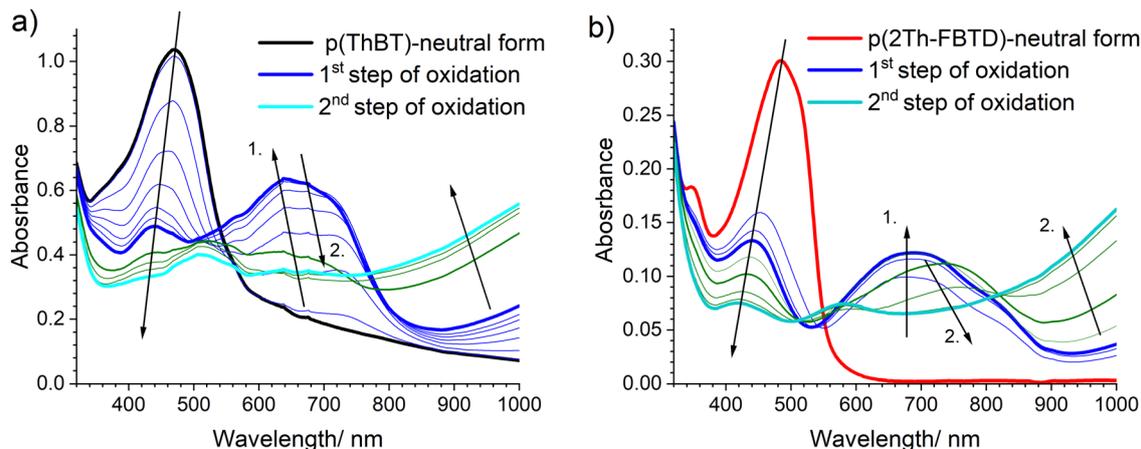
15208 | *J. Mater. Chem. C*, 2024, **12**, 15201–15214

This journal is © The Royal Society of Chemistry 2024

Fig. 10 UV-Vis-NIR spectra collected during electrochemical oxidation of electrodeposited layers in 0.1 M Bu$_4$NPF$_6$/DCM electrolyte. $\uparrow^1$ – absorption growing in intensity during the first oxidation step; $\uparrow^2$ – absorption growing in intensity during the second oxidation step; $\downarrow$ – absorption bands which decrease in intensity during the whole oxidation process; $\downarrow^2$ – absorption bands which decrease in intensity during the second oxidation step.
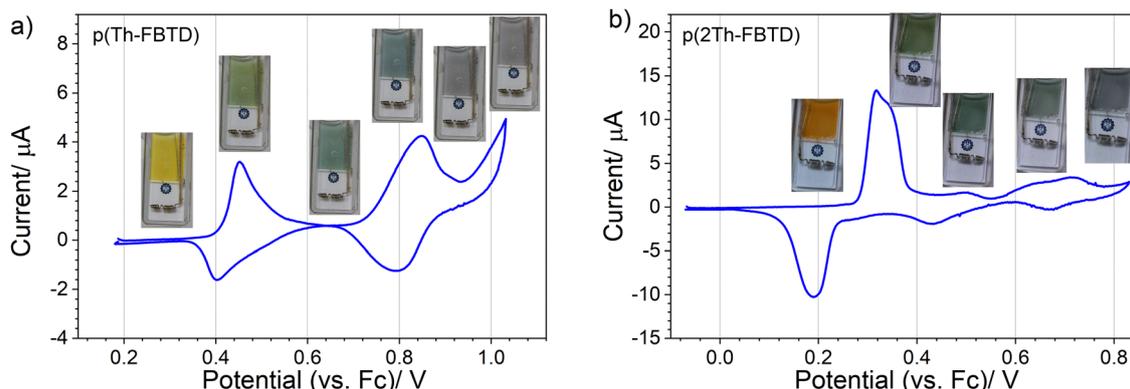

Fig. 11 Cyclic voltammograms of polymer films on ITO electrodes in 0.1 M Bu$_4$NPF$_6$/DCM as the supporting electrolyte solution: (a) **p(Th-FBTD)**; (b) **p(2Th-FBTD)**. Insets: Photographs of polymer films at the given potential. Scan rate 2 mV s^{-1}.

the second oxidation state. During oxidation an equilibrium occurs between partially oxidized (blue) and neutral forms (yellow). Green colour is obtained by combining yellow and blue contributions. The presence of additional thiophene units in **p(2Th-FBTD)** slightly alters the observed electrochromic response. In its neutral state, **p(2Th-FBTD)** is orange, which switches to green upon initial oxidation (first oxidation state), and then to gray upon further oxidation (second oxidation state).

The double potential step chronocoulometric experiment was conducted to characterize the electrochromic reversibility and stability of the thin films. Chronocoulograms, alongside the corresponding alterations in transmittance for **p(Th-FBTD)** and **p(2Th-FBTD)** layers, were recorded during electrochromic switching between neutral and the first oxidized state and are shown in Fig. 12. The outcomes are presented for selected wavelengths representative of the key absorption bands. Basic electrochromic parameters, derived from the experiment, encompassing transmittance difference, optical density difference, charge density, and coloration efficiency were summarized in Table 5.

The analysis of the essential electrochromic parameters, such as optical density and coloration efficiency, clearly indicates differences between **p(Th-FBTD)** and **p(2Th-FBTD)**. The incorporation of additional thiophene units in **p(2Th-FBTD)** improves these parameters in both Vis and NIR ranges. The differences in transmittance between different redox states are greater for **p(2Th-FBTD)** compared to **p(Th-FBTD)**. A similar relation was determined for the charge curves. Both films were obtained from solutions of the same concentration and the same number of oxidation cycles. This may indicate that electrodeposition of **p(2Th-FBTD)** is more efficient than in the case of **p(Th-FBTD)**. Additionally, **p(2Th-FBTD)** most likely shows a stronger UV-Vis absorption compared with **p(Th-FBTD)**. As a result, perhaps, the optical density response of the former is more pronounced. Moreover, the obtained results indicate that **p(2Th-FBTD)** exhibits superior coloration efficiency compared not only to **p(Th-FBTD)** but also to numerous other compounds based on
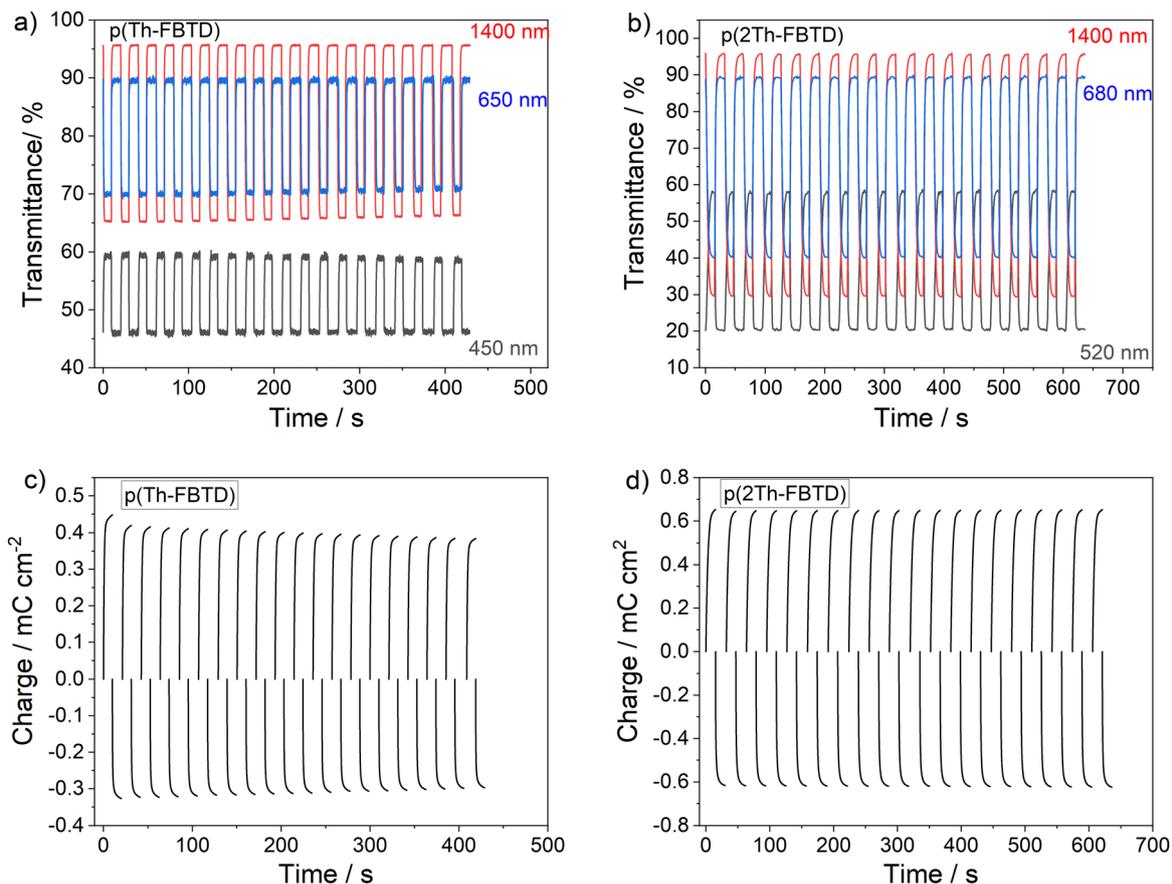
This journal is © The Royal Society of Chemistry 2024

J. Mater. Chem. C, 2024, **12**, 15201–15214 | **15209**

Fig. 12 Kinetic curves recorded during electrochromic switching of polymer films between the neutral and first oxidized states: (a) transmittance of **p(Th-FBTD)**; (b) transmittance of **p(2Th-FBTD)**; (c) chronocoulometry plot for **p(Th-FBTD)**; (d) chronocoulometry plot for **p(2Th-FBTD)**.

Table 5 The electrochromic parameters of **p(Th-FBTD)** and **p(2Th-FBTD)** thin films

Polymer	λ^a/nm	$T_n{}^b$/%	$T_d{}^c$/%	$|\Delta T|^d$/%	$|\Delta OD|^e$	$Q_d{}^f$/mC cm^{-2}	CE^g/cm^2 C^{-1}
p(Th-FBTD)	450	45	59	14	0.12	0.40	297
	650	90	70	20	0.11	0.40	276
	1400	96	65	31	0.17	0.40	428
p(2Th-FBTD)	520	20	58	38	0.46	1.07	432
	680	89	40	49	0.35	1.07	325
	1400	96	29	67	0.52	1.07	485

^{a} Collection wavelength. ^{b} Transmittance of neutral polymer at λ. ^{c} Transmittance of oxidized polymer at λ. ^{d} Transmittance difference between T_n and T_d. ^{e} Optical density difference: $\Delta OD = \log(T_n/T_d)$. ^{f} Charge density. ^{g} Coloration efficiency estimated from equation CE = $|\Delta OD|/Q_d$.

fluorene,[35] thiophene,[36] benzothiadiazole, and other donor–acceptor type polymers known.[37]

Further disparities between the polymer layers of **p(Th-FBTD)** and **p(2Th-FBTD)** are discerned through the analysis of reversibility and stability of transmittance response and chronocoulometric curves recorded during electrochemical switching between the neutral and oxidized state of deposited films. For example, **p(2Th-FBTD)** appears more stable than its counterpart. During 20 consecutive switching cycles, the transmittance response of **p(2Th-FBTD)** film remains nearly invariant, while it gradually diminishes in **p(Th-FBTD)**, indicating inferior electrochemical

stability. Similarly, the recorded chronocoulometric curves of **p(2Th-FBTD)** show much smaller differences than for **p(Th-FBTD)**. Electrochromic behaviour of **p(2Th-FBTD)** is reversible and reproducible in continuous switching cycles as we do not observe a change in the transmittance of neutral and oxidized forms in subsequent switching cycles (Fig. 12b). When the oxidized form is reduced, the transmittance returns to the initial value corresponding to absorption of the neutral form. Similarly, the recorded chronocoulometric curves are virtually invariant during the whole experiment (Fig. 12d). To sum up, comparing **p(2Th-FBTD)** with polymers analogous to fluorene–thiophene–

15210 | *J. Mater. Chem. C*, 2024, **12**, 15201–15214

This journal is © The Royal Society of Chemistry 2024

benzothiadiazole underscores the augmented electrochromic stability of the former.[55]

Conclusions

Two symmetric donor–acceptor–donor (D–A–D) benzothiadiazole derivatives with thiophene (**Th-FBTD**) or bithiophene (**2Th-FBTD**) terminal groups and dihexylfluorene units as linkers between the donor and acceptor parts of the molecule have been synthesized and characterized. Both compounds display relatively high PLQY both in solution (up to 95%) and in the solid state (up to 97%). The studied compounds were employed as emissive dopants in multi-layer solution-processed OLEDs, yielding similar performance with green electroluminescence and an EQE of 3.5% for **Th-FBTD** (Dev 1) and 2.8% for **2Th-FBTD** (Dev 2).

Both compounds undergo quasi-reversible electrochemical reduction and irreversible oxidation. The latter leads to electro-deposition of stable electrochromic layers: **p(Th-FBTD)** and **p(2Th-FBTD)**. The electrodeposited layers undergo reversible one-step electrochemical reduction and two-step reversible oxidation. Analysis reveals that the donor does not significantly affect the electron density of the acceptor, and hence the monomers and their respective polymers display nearly identical LUMO energy. The oxidation potential of **2Th-FBTD** is lower compared to that of **Th-FBTD**, indicating the stronger electron-donating character of bithiophene than the thiophene unit and the respective polymers, **p(2Th-FBTD)** and **p(Th-FBTD)**, following the same trend. It is worth noting that the incorporation of fluorene into the structure of the two monomers has a significant effect on the electrochemical response of the electrodeposited polymeric layers. **p(2Th-FBTD)** and **p(Th-FBTD)** display a significantly higher HOMO than the respective monomers, while the LUMO remains invariant. This stands in stark contrast to instances where thiophenes are directly linked to the acceptor.

Electrochemical oxidation of both electrodeposited layers is accompanied by a reversible color change. Analysis of parameters such as optical density difference and coloration efficiency points out at an improvement of electrochromic properties in both visible and NIR ranges for **p(2Th-FBTD)**, as well as its stability. Furthermore, comparison with other similar fluorene–thiophene–benzothiadiazole polymers reveals the superior electrochromic performance of **p(2Th-FBTD)**.[55] This is crucial to developing stable electrochromic organic materials as they are essential for various photo-electrochemical and optoelectronic applications.[56,57]

A comparative analysis of the OLED devices studied herein reveals performance superior to those previously published, based on active materials capable of electropolymerization and formation of electrochromic polymer films.[58]

Experimental section

Experimental details are available in the ESI,† with details of materials, general procedures and equipment; additional photophysical, and electrochemical data.

Data availability

The data supporting this article have been included as part of the ESI.† Data for this article are available at Zenodo at https://doi.org/10.5281/zenodo.13143794.

Conflicts of interest

There are no conflicts of interest to declare.

Acknowledgements

References

1 S. Soylemez, H. Z. Kaya, Y. A. Udum and L. Toppare, A multipurpose conjugated polymer: Electrochromic device and biosensor construction for glucose detection, *Org. Electron.*, 2019, **65**, 327–333, DOI: 10.1016/j.orgel.2018.11.001.

2 A. Balan, D. Baran and L. Toppare, Benzotriazole containing conjugated polymers for multipurpose organic electronic applications, *Polym. Chem.*, 2011, **2**, 1029–1043, DOI: 10.1039/c1py00007a.

3 D. Baran, A. Balan, S. Celebi, B. Meana Esteban, H. Neugebauer, N. S. Sariciftci and L. Toppare, Processable multipurpose conjugated polymer for electrochromic and photovoltaic applications, *Chem. Mater.*, 2010, **22**, 2978–2987, DOI: 10.1021/cm100372t.

4 C. A. Di, H. Shen, F. Zhang and D. Zhu, Enabling Multifunctional Organic Transistors with Fine-Tuned Charge Transport, *Acc. Chem. Res.*, 2019, **52**, 1113–1124, DOI: 10.1021/acs.accounts.9b00031.

5 H. Shen, A. Abtahi, B. Lussem, B. W. Boudouris and J. Mei, Device Engineering in Organic Electrochemical Transistors toward Multifunctional Applications, *ACS Appl. Electron. Mater.*, 2021, **3**, 2434–2448, DOI: 10.1021/acsaelm.1c00312.

6 L. E. Hueso, I. Bergenti, A. Riminucci, Y. Zhan and V. Dediu, Multipurpose magnetic organic hybrid devices, *Adv. Mater.*, 2007, **19**, 2639–2642, DOI: 10.1002/adma.200602748.

7 S. Tsuneyasu, K. Nakamura and N. Kobayashi, Electroresponsive Dual Functional Display Device Enabling Both Emissive and Reflective Modes by Combining Electrochemiluminescent and Liquid Crystal Materials, *Chem. Lett.*, 2016, **45**, 949–951, DOI: 10.1246/cl.160361.

This journal is © The Royal Society of Chemistry 2024

J. Mater. Chem. C, 2024, **12**, 15201–15214 | **15211**

8 S. Tsuneyasu, L. Jin, K. Nakamura and N. Kobayashi, An electrochemically-driven dual-mode display device with both reflective and emissive modes using poly(p-phenylene-vinylene) derivatives, *Jpn. J. Appl. Phys.*, 2016, **55**, 1–5, DOI: **10.7567/JJAP.55.041601**.

9 S. Tsuneyasu, M. Kawara, K. Enomoto, K. Nakamura and N. Kobayashi, Reflective-emissive representation by combining Ru(ɪɪ)-complex-based electrochemiluminescence and localized- surface-plasmon-resonance-based electrochromism, *Adv. Mater. Technol.*, 2021, **6**, 2000881, DOI: **10.1002/admt.202000881**.

10 M. Gingras, V. Placide, J. M. Raimundo, G. Bergamini, P. Ceroni and V. Balzani, Polysulfurated pyrene-cored dendrimers: Luminescent and electrochromic properties, *Chem. – Eur. J.*, 2008, **14**, 10357–10363, DOI: **10.1002/chem.200801198**.

11 S. Hsiao and N. Liu, Synthesis of blue light emitting and electrochromic polyimidothioethers with diphenylpyrenylamine chromophore via thiol-ene reaction, *J. Polym. Res.*, 2015, **22**, 107, DOI: **10.1007/s10965-015-0754-y**.

12 N. Sun, S. Meng, D. Chao, Z. Zhou, Y. Du, D. Wang, X. Zhao, H. Zhou and C. Chen, Highly stable electrochromic and electrofluorescent dual-switching polyamide containing bis(diphenylamino)-fluorene moieties, *Polym. Chem.*, 2016, **7**, 6055–6063, DOI: **10.1039/c6py01345g**.

13 N. Sun, K. Su, Z. Zhou, X. Tian, Z. Jianhua and D. Chao, High-Performance Emission/Color Dual-Switchable Polymer-Bearing Pendant Tetraphenylethylene (TPE) and Triphenylamine (TPA) Moieties, *Macromolecules*, 2019, **52**, 5131–5139, DOI: **10.1021/acs.macromol.9b00079**.

14 N. Sun, S. Meng, Z. Zhou, J. Yao, Y. Du, D. Wang, X. Zhao, H. Zhou and C. Chen, High-contrast electrochromic and electrofluorescent dual-switching materials based on 2-diphenylamine-(9,9-diphenylfluorene)-functionalized semiaromatic polymers, *RSC Adv.*, 2016, **6**, 66288–66296, DOI: **10.1039/c6ra12174h**.

15 K. Kanazawa, K. Nakamura and N. Kobayashi, Electro-switchable optical device enabling both luminescence and coloration control consisted of fluoran dye and 1,4-benzoquinone, *Sol. Energy Mater. Sol. Cells*, 2016, **145**, 42–53, DOI: **10.1016/j.solmat.2015.06.061**.

16 K. Kanazawa, K. Nakamura and N. Kobayashi, High-contrast electroswitching of emission and coloration based on single-molecular fluoran derivatives, *J. Phys. Chem. A*, 2014, **118**, 6026–6033, DOI: **10.1021/jp5060588**.

17 J. Wu and G. Liou, High-performance electrofluorochromic devices based on electrochromism and photoluminescence-active novel poly(4-cyanotriphenylamine), *Adv. Funct. Mater.*, 2014, **24**, 6422–6429, DOI: **10.1002/adfm.201401608**.

18 H. Al-kutubi, H. Reza, L. Rassaei and K. Mathwig, Electro-fluorochromic systems: Molecules and materials exhibiting redox-switchable fluorescence, *Eur. Polym. J.*, 2016, **83**, 478–498, DOI: **10.1016/j.eurpolymj.2016.04.033**.

19 R. Guermazi, L. Royer, L. Galmiche, G. Clavier, P. Audebert and A. Hedhli, Synthesis and Characterization of New Fluorinated Tetrazines Displaying a High Fluorescence Yield, *J. Fluoresc.*, 2016, 3–10, DOI: **10.1007/s10895-016-1822-3**.

20 P. Audebert and F. Miomandre, Electrofluorochromism: from molecular systems to set-up and display, *Chem. Sci.*, 2013, **4**, 575–584, DOI: **10.1039/c2sc21503a**.

21 U. Koldemir, K. R. Graham, D. H. Salazar, T. D. McCarley and J. R. Reynolds, Electron rich APFO polymer with dual electrochromism and electroluminescence, *J. Mater. Chem.*, 2011, **21**, 6480–6482, DOI: **10.1039/c1jm10345h**.

22 B. B. Carbas, D. Asil, R. H. Friend and A. M. Önal, A new blue light emitting and electrochromic polyfluorene derivative for display applications, *Org. Electron. Phys. Mater. Appl.*, 2014, **15**, 500–508, DOI: **10.1016/j.orgel.2013.12.003**.

23 B. Schmatz, J. F. Ponder and J. R. Reynolds, Multifunctional triphenylamine polymers synthesized via direct (hetero) arylation polymerization, *J. Polym. Sci. Part A Polym. Chem.*, 2018, **56**, 147–153, DOI: **10.1002/pola.28896**.

24 B. Zhao, H. Wang, C. Han, P. Ma, Z. Li and C. P. H. Xu, Highly efficient deep-red non-doped diodes based on a T-shape thermally activated delayed fluorescence emitter, *Angew. Chem., Int. Ed.*, 2020, **59**, 19042–19047, DOI: **10.1002/anie.202008885**.

25 S. Pluczyk, P. Zassowski, C. Quinton, P. Audebert, V. Alain-Rizzo and M. Lapkowski, The influence of the linker on electrochemical and spectroelectrochemical properties of donor-acceptor-donor triphenylamine- *s* -tetrazine derivatives, *Electrochim. Acta*, 2016, **216**, 160–170, DOI: **10.1016/j.electacta.2016.09.009**.

26 S. Pluczyk, P. Zassowski, R. Rybakiewicz, R. Wielgosz, M. Zagorska, M. Lapkowski and A. Pron, UV-vis and EPR spectroelectrochemical investigations of triarylamine functionalized arylene bisimides, *RSC Adv.*, 2015, **5**, 7401–7412, DOI: **10.1039/C4RA12603C**.

27 Z. Li, D. Yand, C. Han, B. Zhao, H. Wang, Y. Man, P. Ma, P. Chang, D. Ma and H. Xu, Optimizing hharge transfer and out-coupling of a quasi-planar deep-red TADF emitter: towards Rec.2020 Gamut and external quantum efficiency beyond 30%, *Angew. Chem., Int. Ed.*, 2021, **60**, 14846–14851, DOI: **10.1002/anie.202103070**.

28 S. Nasiri, S. Macionis, D. Gudeika, D. Volyniuk and J. V. Grazulevicius, Facile structure-modification of xanthenone based OLED emitters exhibiting both aggregation induced emission enhancement and thermally activated delayed fluorescence, *J. Lumin.*, 2020, **220**, 116955, DOI: **10.1016/j.jlumin.2019.116955**.

29 T. E. A. Frizon, J. C. Valdivia Martínez, J. L. Westrup, R. da, C. Duarte, E. Zapp, K. G. Domiciano, F. S. Rodembusch and A. G. Dal-Bó, 2,1,3-Benzothiadiazole-based fluorophores, Synthesis, electrochemical, thermal and photophysical characterization, *Dyes Pigm.*, 2016, **135**, 26–35, DOI: **10.1016/j.dyepig.2016.07.011**.

30 A. Pathak, K. R. Justin Thomas, M. Singh and J. H. Jou, Fine-Tuning of Photophysical and Electroluminescence Properties of Benzothiadiazole-Based Emitters by Methyl Substitution, *J. Org. Chem.*, 2017, **82**, 11512–11523, DOI: **10.1021/acs.joc.7b02127**.

31 S. W. Huang and K. C. Ho, An all-thiophene electrochromic device fabricated with poly(3-methylthiophene) and

15212 | *J. Mater. Chem. C*, 2024, **12**, 15201–15214

This journal is © The Royal Society of Chemistry 2024

poly(3,4-ethylenedioxythiophene), *Sol. Energy Mater. Sol. Cells*, 2006, **90**, 491–505, DOI: **10.1016/j.solmat.2005.02.016**.

32 M. Chang, W. Chen, H. Xue, D. Liang, X. Lu and G. Zhou, Conjugation-extended viologens with thiophene derivative bridges: Near-infrared electrochromism, electrofluorochromism, and smart window applications, *J. Mater. Chem. C*, 2020, **8**, 16129–16142, DOI: **10.1039/d0tc03680c**.

33 F. Fabrizi De Biani, A. Reale, V. Razzano, M. Paolino, G. Giuliani, A. Donati, G. Giorgi, W. Mróz, D. Piovani, C. Botta and A. Cappelli, Electrochemical and optoelectronic properties of terthiophene- and bithiophene-based polybenzofulvene derivatives, *RSC Adv.*, 2018, **8**, 10836–10847, DOI: **10.1039/c7ra13242e**.

34 S. Yan, Y. Dong, W. Li, L. Chen, Y. Dai, N. Ren, Y. Wu, Y. Zhang and C. Zhang, Electrochemical and electrochromic properties of bilayer polymer films prepared by electrochemical polymerization based on star-shaped thiophene derivatives, *New J. Chem.*, 2019, **43**, 9566–9573, DOI: **10.1039/c9nj01730e**.

35 B. Bezgin Carbas, Fluorene based electrochromic conjugated polymers: A review, *Polymer*, 2022, **254**, 125040, DOI: **10.1016/j.polymer.2022.125040**.

36 T. Moreira, F. Di Maria, M. Zangoli, E. Fabiano, I. Manet, R. Mazzaro, V. Morandi, M. Marinelli, G. Gigli, A. J. Parola, C. A. T. Laia and G. Barbarella, Processable Thiophene-Based Polymers with Tailored Electronic Properties and their Application in Solid-State Electrochromic Devices Using Nanoparticle Films, *Adv. Electron. Mater.*, 2021, **7**, 2100166, DOI: **10.1002/aelm.202100166**.

37 X. Lv, W. Li, M. Ouyang, Y. Zhang, D. S. Wright and C. Zhang, Polymeric electrochromic materials with donor–acceptor structures, *J. Mater. Chem. C*, 2017, **5**, 12–28, DOI: **10.1039/C6TC04002K**.

38 E. Taylor-Shaw, E. Angioni, N. J. Findlay, B. Breig, A. R. Inigo, J. Bruckbauer, D. J. Wallis, P. J. Skabara and R. W. Martin, Cool to warm white light emission from hybrid inorganic/organic light-emitting diodes, *J. Mater. Chem. C*, 2016, **4**, 11499–11507, DOI: **10.1039/c6tc03585J**.

39 H. H. Huang, C. Prabhakar, K. C. Tang, P. T. Chou, G. J. Huang and J. S. Yang, Ortho-branched ladder-type oligophenylenes with two-dimensionally π-conjugated electronic properties, *J. Am. Chem. Soc.*, 2011, **133**, 8028–8039, DOI: **10.1021/ja202144v**.

40 F. Neese, Software update: the ORCA program system, version 4.0, *WIREs Comput. Mol. Sci.*, 2018, **8**, e1327, DOI: **10.1002/wcms.1327**.

41 F. Neese, The ORCA program system, *Wiley Interdiscip. Rev.: Comput. Mol. Sci.*, 2012, **2**, 73–78, DOI: **10.1002/wcms.81**.

42 S. Lehtola, C. Steigemann, M. J. T. Oliveira and M. A. L. Marques, Recent developments in libxc—A comprehensive library of functionals for density functional theory, *SoftwareX*, 2018, **7**, 1–5, DOI: **10.1016/j.softx.2017.11.002**.

43 S. J. Strickler and R. A. Berg, Relationship between absorption intensity and fluorescence lifetime of molecules, *J. Chem. Phys.*, 1962, **37**, 814–822, DOI: **10.1063/1.1733166**.

44 T. Matulaitis, N. Kostiv, J. V. Grazulevicius, L. Peciulyte, J. Simokaitiene, V. Jankauskas, B. Luszczynska and J. Ulanski, Synthesis and properties of bipolar derivatives of 1,3,5-triazine and carbazole, *Dyes Pigm.*, 2016, **127**, 45–58, DOI: **10.1016/j.dyepig.2015.11.001**.

45 A. Belyaev, S. O. Slavova, I. V. Solovyev, V. V. Sizov, J. Jänis, V. Grachova and I. O. Koshevoy, Solvatochromic dual luminescence of Eu – Au dyads decorated with chromophore phosphines, *Inorg. Chem. Front.*, 2020, **7**, 140–149, DOI: **10.1039/c9qi01015g**.

46 Y. Chen, J. Zhao, H. Guo and L. Xie, Geometry relaxation-induced large Stokes shift in red-emitting borondipyrromethenes (BODIPY) and applications in fluorescent thiol probes, *J. Org. Chem.*, 2012, **77**, 2192–2206, DOI: **10.1021/jo202215x**.

47 Y. Xu, Z. Cheng, Z. Li, B. Liang, J. Wang, J. Wei, Z. Zhang and Y. Wang, Molecular-structure and device-configuration optimizations toward highly efficient green electroluminescence with narrowband emission and high color purity, *Adv. Opt. Mater.*, 2020, **8**, 1902142, DOI: **10.1002/adom.201902142**.

48 S. A. Ahmad, J. Eng and T. J. Penfold, Rapid predictions of the colour purity of luminescent organic molecules, *J. Mater. Chem. C*, 2022, **10**, 4785–4794, DOI: **10.1039/d1tc04748e**.

49 P. Ledwon, N. Thomson, E. Angioni, N. J. Findlay, P. J. Skabara and W. Domagala, The role of structural and electronic factors in shaping the ambipolar properties of donor-acceptor polymers of thiophene and benzothiadiazole, *RSC Adv.*, 2015, **5**, 77303–77315, DOI: **10.1039/c5ra06993a**.

50 R. Pashazadeh, P. Pander, A. Lazauskas, F. B. Dias and J. V. Grazulevicius, Multicolor Luminescence Switching and Controllable Thermally Activated Delayed Fluorescence Turn on/Turn off in Carbazole-Quinoxaline-Carbazole Triads, *J. Phys. Chem. Lett.*, 2018, **9**, 1172–1177, DOI: **10.1021/acs.jpclett.8b00136**.

51 Y. Wei, C. C. Chan, J. Tian, G. W. Jang and K. F. Hsueh, Electrochemical Polymerization of Thiophenes in the Presence of Bithiophene or Terthiophene: Kinetics and Mechanism of the Polymerization, *Chem. Mater.*, 1991, **3**, 888–897, DOI: **10.1021/cm00017a026**.

52 J. Roncali, Conjugated Poly(thiophenes): Synthesis, Functionalization, and Applications, *Chem. Rev.*, 1992, **92**, 711–738, DOI: **10.1021/cr00012a009**.

53 K. R. Idzik, P. Ledwon, R. Beckert, S. Golba, J. Frydel and M. Lapkowski, Electrochemical and spectral properties of meta-linked 1,3,5-tris(aryl) benzenes and 2,4,6-tris(aryl)-1-phenoles, and their polymers, *Electrochim. Acta*, 2010, **55**, 7419–7426, DOI: **10.1016/j.electacta.2010.07.005**.

54 P. Audebert, J. M. Catel, G. Le Coustumer, V. Duchenet and P. Hapiot, Electrochemistry and polymerization mechanisms of thiophene-pyrrole-thiopnene oligomers and terthiophenes. Experimental and theoretical modeling studies, *J. Phys. Chem. B*, 1998, **102**, 8661–8669, DOI: **10.1021/jp9804289**.

55 C. Z. Karaman, S. Göker, Ü. Şahin, S. O. Hacioglu, S. T. Aslan, T. Hacıefendioğlu, G. Hizalan, E. Yıldırım, A. Çırpan and L. Toppare, Effect of thiophene, 3-hexylthiophene, selenophene, and Thieno[3,2-b]thiophene spacers on OPV device performance of novel 2,1,3-benzothiadiazole based

This journal is © The Royal Society of Chemistry 2024

J. Mater. Chem. C, 2024, **12**, 15201–15214 | **15213**

alternating copolymers, *J. Electroanal. Chem.*, 2021, **895**, 115483, DOI: **10.1016/j.jelechem.2021.115483**.

56 L. Scalon, A. Leithold Neto, L. O. Araujo, S. Zaioncz, J. B. Floriano, A. G. Macedo, C. M. Araujo, C. F. N. Marchiori and P. C. Rodrigues, Assessing the Donor–Acceptor Nature and the Electrochemical Stability of a Fluorene–Diketopyrrolopyrrole–Thiophene-Based Copolymer, *ACS Appl. Polym. Mater.*, 2021, **3**, 4223–4233, DOI: **10.1021/acsapm.1c00651**.

57 J. Jensen, M. V. Madsen and F. C. Krebs, Photochemical stability of electrochromic polymers and devices, *J. Mater. Chem. C*, 2013, **1**, 4826–4835, DOI: **10.1039/c3tc30751d**.

58 S. Koyuncu, O. Usluer, M. Can, S. Demic, S. Icli and N. Serdar Sariciftci, Electrochromic and electroluminescent devices based on a novel branched quasi-dendric fluorene-carbazole-2,5-bis(2-thienyl)-1H-pyrrole system, *J. Mater. Chem.*, 2011, **21**, 2684–2693, DOI: **10.1039/c0jm02366c**.

15214 | *J. Mater. Chem. C*, 2024, **12**, 15201–15214

This journal is © The Royal Society of Chemistry 2024